Palaeogeography, Palaeoclimatology, Palaeoecology 475 (2017) 115–124

Contents lists available at ScienceDirect

Palaeogeography, Palaeoclimatology, Palaeoecology

journal homepage: www.elsevier.com/locate/palaeo

A record of Holocene sea-ice variability off West Greenland and its potential forcing factors

Longbin Sha [a,*], Hui Jiang [b], Marit-Solveig Seidenkrantz [c], Dongling Li [a], Camilla S. Andresen [d], Karen Luise Knudsen [c], Yanguang Liu [e], Meixun Zhao [f]

[a] Department of Geography & Spatial Information Techniques, Ningbo University, 315211 Ningbo, PR China
[b] Key Laboratory of Geographic Information Science, East China Normal University, 200062 Shanghai, PR China
[c] Centre for Past Climate Studies and Arctic Research Centre, Department of Geoscience, Aarhus University, DK-8000 Aarhus C, Denmark
[d] Geological Survey of Denmark and Greenland, Department of Marine Geology and Glaciology, Øster Voldgade 10, 1350 Copenhagen K, Denmark
[e] Key Laboratory of Marine Sedimentology and Environmental Geology, First Institute of Oceanography, SOA, 266061 Qingdao, PR China
[f] Key Laboratory of Marine Chemistry Theory and Technology, Ministry of Education, Ocean University of China, 266100 Qingdao, PR China

ARTICLE INFO

Article history:
Received 6 October 2016
Received in revised form 12 March 2017
Accepted 20 March 2017
Available online 21 March 2017

Keywords:
Sea-ice concentration
Diatoms
Solar forcing
Ocean circulation

ABSTRACT

We present a reconstruction of Holocene sea-ice variability from sediment core GA306-GC3, from the Holsteinsborg Dyb off West Greenland, which provides an index of palaeoceanographic and palaeoenvironmental conditions within this climatically sensitive region during the last 6700 yr. The reconstructed sea-ice record, combined with previously published proxy data, suggests that relatively warm conditions with reduced sea-ice extent prior to 5000 cal. yr BP were associated with the Holocene Thermal Maximum. Subsequent cooling and extensive sea-ice cover between ca. 5000 and 4000 cal. yr BP was followed by even colder conditions and persistent sea-ice cover during the Neoglacial cooling phase, particularly after ca. 1500 cal. yr BP. There is a positive correlation between West Greenland sea-ice cover and solar activity over the past 5000 yr, but the correlation is much weaker prior to 5000 cal. yr BP. In addition, there is a strong link between West Greenland sea ice and changes in the abundance of arctic benthic foraminifera species, related to different water masses of the West Greenland Current during the entire interval, even prior to 5000 cal. yr BP. Our findings indicate that sea-ice variability off West Greenland was driven not only by solar activity, but also by ocean circulation (the strength of cold Polar water from the East Greenland Current and warm Atlantic water from the Irminger Current).

1. Introduction

Arctic sea ice is an important component of global climate and of the atmospheric and marine circulation systems, and plays a critical role in high latitude ecosystems and marine carbon cycling. For example, sea ice insulates the polar oceans from the atmosphere and consequently influences the exchange of heat, gases and moisture between them. During the past few decades, the extent and thickness of summer Arctic sea ice has decreased abruptly (Kinnard et al., 2011; NSIDC, 2016), and model simulations suggest that Arctic summer sea ice may disappear within the next fifty or even thirty years (Holland et al., 2006; Wang and Overland, 2012; Stroeve et al., 2012). Given the magnitude of the ongoing reduction of Arctic sea ice, it is crucial to obtain a clear and detailed picture of past sea-ice variations and the controlling factors. However, systematic satellite measurements of Arctic sea-ice only began in late 1978 and since predictive climate models rely on historical records there is a widely accepted need for high-resolution proxy records of past variations in sea-ice cover (Jones et al., 2001; Massé et al., 2010).

Various proxies have been used to reconstruct past changes in Arctic sea-ice conditions (Belt and Müller, 2013; Belt et al., 2007; Cabedo-Sanz et al., 2016; de Vernal and Hillaire-Marcel, 2000; de Vernal et al., 2013a, 2013b; Funder et al., 2011; Justwan and Koç Karpuz, 2008; Müller et al., 2011, 2012; Massé et al., 2008; Miettinen et al., 2015; Seidenkrantz, 2013; Sha et al., 2014; Weckström et al., 2013). Among these, diatoms, marine siliceous algae, have been used successfully for the reconstruction of sea-ice concentration in the Arctic region, such as off West Greenland during the late Holocene (Sha et al., 2014) and the last millennium (Sha et al., 2016); off Southeast Greenland over the past 2900 yr (Miettinen et al., 2015); and off Iceland during the Holocene (Justwan and Koç Karpuz, 2008) and the last 1000 yr (Sha et al., 2015).

The West Greenland shelf is influenced by the northward-flowing West Greenland Current (WGC), which consists of two components of different origin: Polar Water from the Arctic Ocean delivered by the East Greenland Current (EGC) and Atlantic-sourced water derived from the Irminger Current (IC) (Fig. 1) (Buch et al., 2001; Cuny et al.,

* Corresponding author.
E-mail address: shalongbin@nbu.edu.cn (L. Sha).

http://dx.doi.org/10.1016/j.palaeo.2017.03.022
0031-0182/

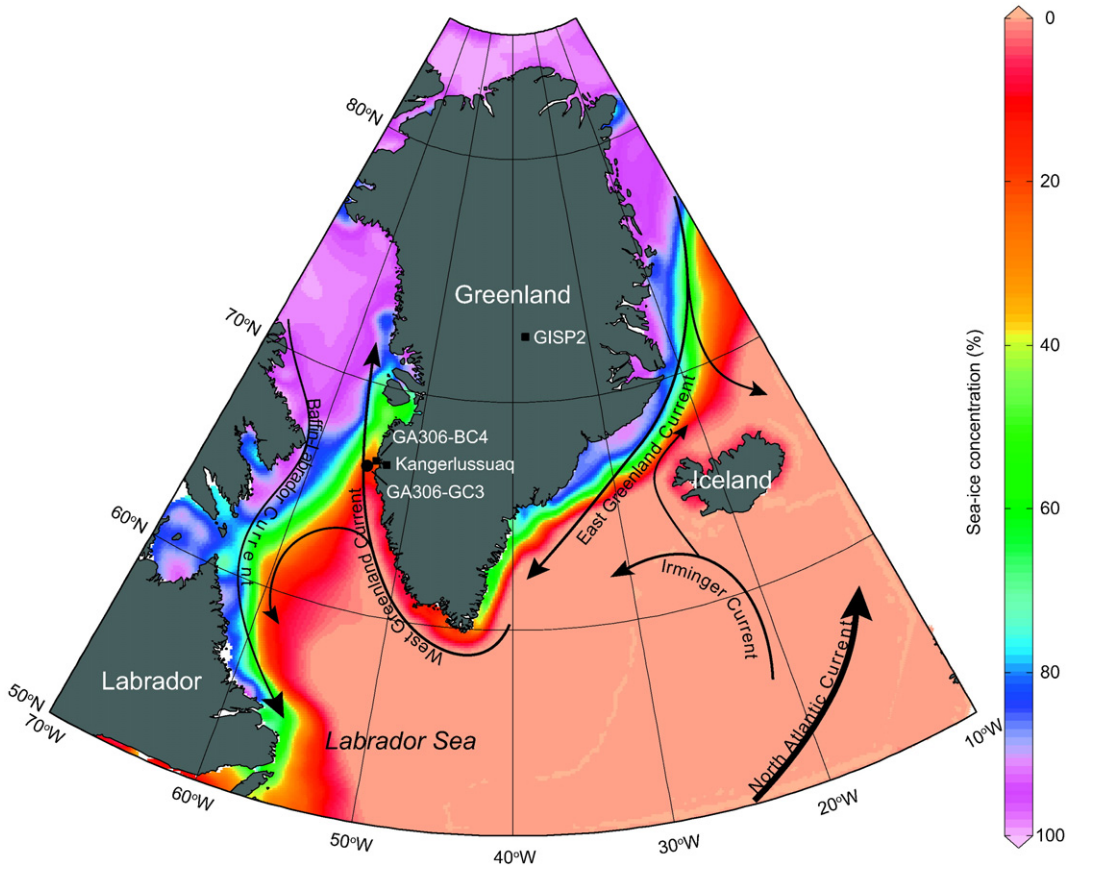

Fig. 1. Location of marine sediment core GA306-GC3 and the other palaeoclimatic records referenced in the text, together with the modern surface circulation of the North Atlantic. The satellite April sea-ice concentration from Nimbus-7 SMMR and DMSP SSM/I-SSMIS Passive Microwave Data (GSFC product, NSIDC-0051) for the interval from CE 1979–2010 is also indicated. The map was generated with Ocean Data View (Schlitzer, 2011).

2002; Tang et al., 2004). In addition, the shelf is dominated by two different types of sea ice: multi-year ice transported from the Arctic Ocean by the EGC and first-year ice formed in Baffin Bay, the Davis Strait and the western part of the Labrador Sea (Buch, 2000). During winter and spring, sea ice normally covers most of Davis Strait north of 65 °N. South of 65–67 °N, the eastern Labrador Sea is mainly free of sea ice (NSIDC, 2016; compilation in Seidenkrantz, 2013), but sea ice may occur for short intervals during late winter or during spring and the early summer months if multi-year ice originating from the Arctic Ocean and Fram Strait drifts into the area via the EGC (Hansen et al., 2004; Sha et al., 2016). Since our studied shelf area off Kangerlussuaq is located at the boundary between the area of relatively extensive sea-ice cover to the north and almost sea-ice free water to the south, it is highly sensitive to climate change in general and to sea-ice variability in particular (Fig. 1). Despite its important location, there is a paucity of high-resolution and long-term (Holocene) sea-ice reconstructions for this climatically sensitive region.

A link between solar forcing and sea-ice variability off West Greenland during the last millennium has been demonstrated (Sha et al., 2016). Decreased solar irradiance would have induced cooling and increased sea-ice extent in the entire Arctic region (Moffa-Sánchez et al., 2014). In addition, ocean circulation likely also played a significant role for the response of sea ice to the solar forcing during the last 1000 yr (Sha et al., 2015). However, due to the relatively short time spans addressed by previous studies, it is necessary to clarify whether or not these relationships persisted throughout the Holocene, and to assess the importance of external forcing mechanisms such as solar irradiance compared to internal mechanisms.

The aim of the present study is to gain insights into the spatiotemporal variation of sea-ice during the past 7000 yr, by applying a diatom transfer function to gravity core GA306-GC3, a well-dated high-resolution marine sediment record from off West Greenland (Erbs-Hansen et al., 2013). In order to evaluate the relationship between sea-ice variability off West Greenland and the climate of the adjacent areas, we compare our record with an alkenone-based lake temperature record from the Kangerlussuaq region (D'Andrea et al., 2011), and with the GISP2 ice core temperature record from Greenland (Alley, 2000; Cuffey and Clow, 1997). In addition, in order to assess the possible influence of different forcing factors on sea-ice variability, we compare our sea-ice reconstruction with the cosmogenic nuclide ^{14}C record obtained from tree-rings (Muscheler et al., 2007; Reimer et al., 2009), and with species assemblages of selected benthic foraminifera from the same core (Erbs-Hansen et al., 2013), which reflect the different water masses of the WGC.

2. Materials and methods

2.1. Diatom data

Gravity core GA306-GC3 (66°37′29″N, 54°12′35″W; 440-cm long) was retrieved from a water depth of 425 m in the Holsteinsborg Dyb Basin off Kangerlussuaq, West Greenland, during the Galathea 3 Expedition, Leg 3, 25 August to 8 September 2006 (Fig. 1). Diatom analyses were conducted on 1-cm thick slices taken at 5-cm intervals from the core, yielding a mean temporal resolution of ca. 70 yr. The samples were freeze-dried and ca. 0.5 g of dry sediment was treated with 10% HCl to remove carbonates and with 30% H_2O_2 (3 h in a water bath at 70 °C) to remove organic material. Subsequently, the samples were rinsed with distilled water via a cycle of sedimentation and decantation until no acid remained. An aliquot of shaken suspension was placed on a

cover slip and mixed with a pipette in order to achieve a uniform distribution of diatoms on the cover slip. After the material had completely dried, cover slips were transferred onto permanently labeled slides, mounted with Naphrax (refraction index = 1.73) and heated to 250 °C. For each sample, at least 300 diatom valves (excluding *Chaetoceros* resting spores) were identified and counted using a Leica microscope at 1000× magnification. Diatoms were identified to species or species group level following the standard taxonomical literature for marine diatoms (Cremer, 1998; Hasle and Syvertsen, 1997; Medlin and Priddle, 1990; Witkowski et al., 2000). Diatom relative abundances were calculated as percentage of all diatom taxa excluding *Chaetoceros* resting spores with the prediction error for each sample calculated using the program C2, which combines the standard error of estimates for each samples with the error in the calibration function.

2.2. Chronology

In order to establish a chronology for gravity core GA306-GC3, 15 samples of extracted marine mollusc shells were measured for their radiocarbon content at the AMS ^{14}C Dating Centre, Aarhus University, Denmark (see Table 1). All of the dates are calibrated using the Marine09 ^{14}C calibration dataset (Reimer et al., 2009) with a ΔR of 140 ± 30 yr (Erbs-Hansen et al., 2013, McNeely et al., 2006). Data from a box core at the same core site were included for the constructing the top part of the age-depth model (see Erbs-Hansen et al., 2013). The ^{14}C-based chronology was constructed using the depositional model option in OxCal 4.1 software (Ramsey, 2009) with a *k* value of 130 (see Fig. 2). The resulting age model indicates that core GA306-GC3 spans the time interval from ca. 6700–130 cal. yr BP.

2.3. Transfer function for palaeo-sea-ice concentration

Diatoms are useful indicators of past climatic and environmental changes because they occur widely in marine/lacustrine environments and are highly sensitive to ambient ecological conditions (Jiang et al., 2001, 2005, 2015; Koç Karpuz and Schrader, 1990; Reed et al., 2012). Quantitative palaeo-sea-ice conditions can be reconstructed by applying a transfer function to down-core diatom assemblages. The approach has been used successfully for quantitatively reconstructing past sea-ice conditions in the North Atlantic (Justwan and Koç Karpuz, 2008; Miettinen et al., 2015; Sha et al., 2014). A modern calibration data set, consisting of 72 surface sediment samples from Baffin Bay, Davis Strait, Labrador Sea and from around Iceland, has been created for quantitative reconstruction of April sea-ice concentration in the study area (Sha et al., 2014). Seven transfer function methods were tested and a weighted

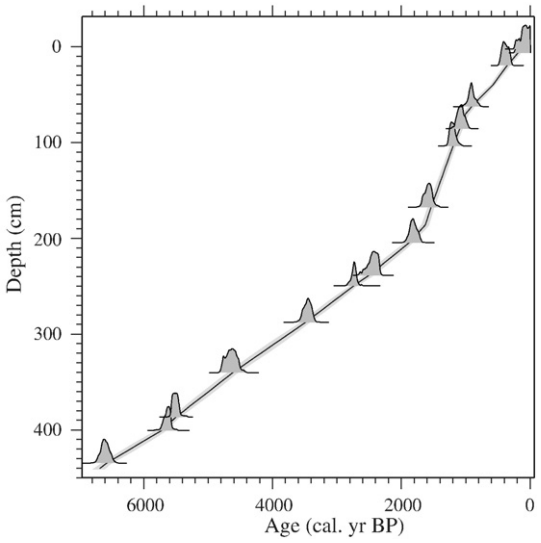

Fig. 2. Age-depth model for core GA306-GC3 (for detailed information see Erbs-Hansen et al., 2013).

averaging with partial least squares regression (WA-PLS) using 3 components (which has the lowest root-mean squared error of prediction based on the leave-one-out jack-knifing $RMSEP_{(Jack)}$ of 1.065 and the highest coefficient of determination between observed and predicted values R^2_{Jack} of 0.916) was selected to quantitatively reconstruct palaeo-sea-ice changes (Sha et al., 2014). It has been shown that a reconstructed April sea-ice record for the last ca. 75 yr using the same transfer function from nearby box core GA306-BC4 (Fig. 1) is in good agreement with satellite sea-ice concentration data (Sha et al., 2014).

2.4. Time series analysis

The statistical significance of the correlation between changes in the sea-ice concentration and ^{14}C production rate, as well as species assemblages of selected benthic foraminifera, was evaluated using comparisons with synthetic red-noise time series (Knudsen et al., 2014). The synthetic data were modelled as an AR1 process following the procedure of Schulz and Mudelsee (2002) with characteristic memory factors (ϕ) equal to that obtained for the raw, unfiltered sea-ice concentration data. The characteristic memory factor (ϕ) was obtained using the covariance function for the AR1 process given as $\mathrm{cov}(X(t_i), X(t_j)) = \Phi_0 \times \phi^{|j-i|}$, where Φ_0 is the variance and $\mathrm{cov}(X(t_i), X(t_j))$ is the

Table 1
AMS ^{14}C age determinations for gravity core GA306-GC3.

Laboratory code	Material (mollusc shell)	Depth (cm)	δ^{13}C (‰)	δ^{18}O (‰)	Age (^{14}C yr BP)	Modelled age (cal. yr BP)
AAR-11282	*Thyasira gouldi*	2–3	−3.94	−9.45	613 ± 29	n/a
AAR-14532	*Megayoldia thraciaeformis*	6–7	0.31	3.64	606 ± 24	n/a
AAR-11284	*Thyasira gouldi*	19–20	−3.81	−8.76	889 ± 28	430–305 (105.9%)
AAR-11286	*Thyasira gouldi*	62–63	−2.63	−8.10	1507 ± 29	968–828 (123.1%)
AAR-14533	*Ciliatocardium ciliatum*	85–86	1.54	3.13	1664 ± 23	1158–1025 (119.9%)
AAR-11287	*Megayoldia thraciaeformis*	103–104	0.51	−7.88	1783 ± 26	1255–1134 (112.2%)
AAR-11288	*Nuculana pernula costigera*	167–168	0.77	−7.8	2156 ± 31	1614–1440 (100.3%)
AAR-11289	*Thyasira gouldi*	204–205	−1.53	−8.31	2356 ± 31	1962–1797 (81.0%)
AAR-14534	*Yoldia* cf. *hyperborea*	238–239	0.03	3.61	2873 ± 24	2605–2396 (82.7%)
AAR-11290	*Macoma moesta*	249–250	0.86	−7.42	3097 ± 31	2808–2677 (115.2%)
AAR-11291	*Yoldiella lenticula*	287–288	0.86	−8.56	3706 ± 33	3571–3385 (102.7%)
AAR-11292	*Yoldiella lenticula*	340	1.38	2.06	4595 ± 39	4739–4501 (109.4%)
AAR-14535	*Megayoldia thraciaeformis*	386–387	−0.11	3.59	5278 ± 27	5573–5436 (107.4%)
AAR-11293	*Yoldiella hyperborea*	400–401	−2.03	−7.62	5409 ± 38	5836–5630 (48.1%)
AAR-11294	*Liocyma fluctuosum*	434–435	−0.35	−7.62	6306 ± 38	6680–6458 (98.7%)

The ^{14}C ages are calibrated with OxCal 4.1 software (Ramsey, 2009) using the Marine09 calibration data set (Reimer et al., 2009) with a ΔR of 140 ± 30 yr (Erbs-Hansen et al., 2013). Modelled age is shown with the 95.4% confidence interval. The agreement index, denoting the overlap between the likelihood probability of the unmodelled calibrated probability distribution and the modelled probability distribution, is provided in brackets. Modelled ages marked with n/a were not used in the age model.

covariance observed at |j-i| time steps from zero lag. A total of 10,000 synthetic sea-ice concentration data sets were simulated using a Monte Carlo approach, and the correlation coefficients obtained between the synthetic sea-ice concentration data and ^{14}C production rate, as well as selected benthic foraminifera species, were compared to those obtained for the actual sea-ice concentration data. In addition, the wavelet-transform-based technique was used for band-pass filtering (Torrence and Compo, 1998).

3. Results and discussion

3.1. Reconstructed sea-ice concentration during the Holocene

We applied the diatom-based sea-ice transfer function to the diatom data from core GA306-GC3 in order to establish a sea-ice record for the last ca. 6700 yr. The reconstructed sea-ice concentration off West Greenland varied between 15 and 60% during this interval (Fig. 3). The prediction error for each fossil sample ranges between 3.29% and 11.36%. Prior to 5000 cal. yr BP, the sea-ice concentration ranged from 15 to 40% with an average of about 28% - close to the present-day value (Figs. 1 and 3). The pre-5000 cal. yr BP interval is characterized by relatively low frequencies of sea-ice diatom species (*Fragilariopsis cylindrus*, *Fossula arctica*, *Detonula confervaceae* resting spore and *Bacterosira bathyomphala*) (e.g. Bauch and Polyakova, 2000; Hasle and Syvertsen, 1997; Jensen, 2003; Krawczyk et al., 2010; von Quillfeldt, 1996), low abundances of cold-water diatom species (*Thalassiosira nordenskioeldii*, *Thalassiosira antarctica* var. *borealis* resting spore, *Thalassiosira antarctica* vegetative cells and *Thalassiosira hyalina*) (Hasle and Syvertsen, 1997; Jensen, 2003; Sha et al., 2014) and by high abundances of warm-water diatom taxa (*Thalassionema nitzschioides*, *Thalassiosira oestrupii*, *Rhizosolenia hebetata* f. *semispina* and *Rhizosolenia borealis*) (Hasle and Syvertsen, 1997; Jiang et al., 2001; Koç Karpuz and Schrader, 1990; Sha et al., 2014) (Fig. 3). An extensive sea-ice cover occurred from 5000 to 4100 cal. yr BP. Increased abundances of sea-ice and cold-water diatom species, and a decrease in warm-water diatom species, also indicate relatively cold surface water conditions from 5000 to 4100 cal. yr BP. After a subsequent period of low sea-ice values from 4100 to 2900 cal. yr BP, relatively high, but varying sea-ice values occurred again between ca. 2900 and 2000 cal. yr BP. This is reflected in the diatom data by an increase in

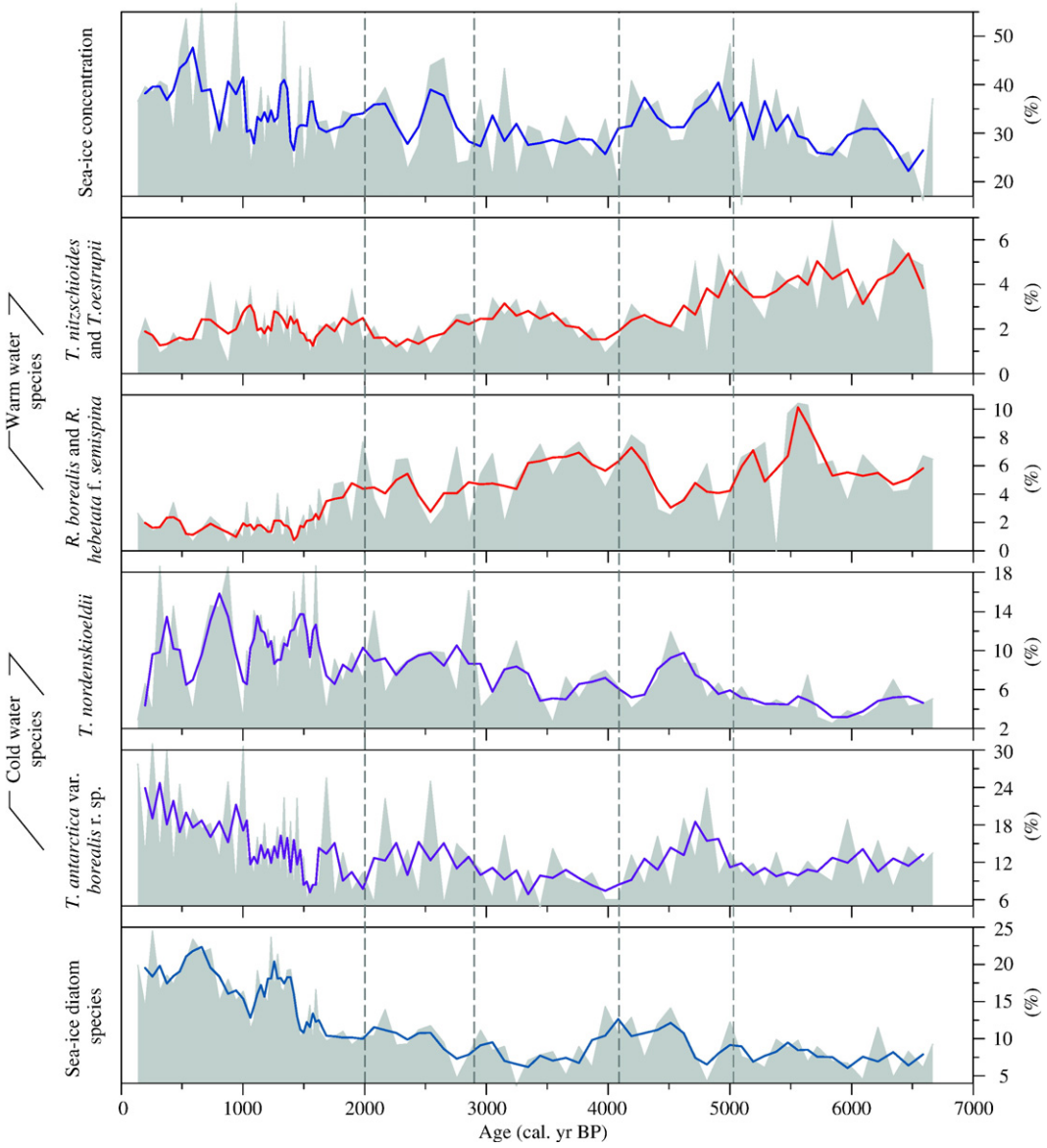

Fig. 3. Relative abundances of the most common diatom species from core GA306-GC3 and diatom-based reconstructed sea-ice concentration from the same site. Smoothed records (3-point running average) are denoted by bold black lines. The vertical dashed line indicates the boundary between different climatic intervals as suggested by the diatom assemblages.

cold-water and sea-ice species (Fig. 3). After ca. 1750 cal. yr BP, sea-ice cover expanded again, particularly after ca. 1500 cal. yr BP, except for short intervals of somewhat reduced sea ice at around 1000 cal. yr BP (Fig. 3). This general increase in sea-ice cover is shown by a significant increase in sea-ice diatom species (*F. cylindrus*, *F. arctica*, *D. confervaceae* resting spore and *B. bathyomphala*), and by a marked decline or even disappearance of warm-water diatom species (Fig. 3).

3.2. Comparison with palaeoclimatic records from adjacent areas

The overall pattern of our sea-ice reconstruction (Fig. 4a) is in general agreement with the alkenone-based temperature reconstruction from two lakes in the Kangerlussuaq region, close to our study site (D'Andrea et al., 2011) (Fig. 4b), and with the temperature record from the GISP2 ice core from Greenland Summit (Alley, 2000; Cuffey and Clow, 1997) (Fig. 4c) (Supplementary Figs. S4 and S5). The Kangerlussuaq lake temperature record exhibits a cooling trend between 5600 and 5000 cal. yr BP and a subsequent cold interval between 5000 and 4100 cal. yr BP. High lake temperatures occurred at about 4000–3000 cal. yr BP, followed by the Neoglacial cooling at ca. 3000 cal. yr BP. The Kangerlussuaq lake records also reveal a change to relatively cold conditions after ca. 1750 cal. yr BP, coinciding with a similar change in our sea-ice reconstruction. The GISP2 temperature record from Greenland Summit exhibits a generally similar overall trend (Fig. 4), with higher temperatures between 4100 and 3200 cal. yr BP, gradually decreasing temperatures after ca. 3100 cal. yr BP, and low temperatures after ca. 1500 cal. yr BP, interrupted by an increase during a short interval around 1000 cal. yr BP.

As demonstrated above, all of the three records indicate warm conditions before about 5000 cal. yr BP, corresponding in time to the Holocene Thermal Maximum. However, the exact timing of the Holocene Thermal Maximum varies spatially across the North Atlantic and Greenland region (e.g. Gajewski, 2015; Kaplan et al., 2002; Kaufman et al., 2004; Larsen et al., 2015). Off West Greenland, Funder and Weidick (1991) identified the Holocene Thermal Maximum based on boreal mollusc shells during the interval 8400–4900 ^{14}C yr BP (9200–5500 cal. yr BP). In Kangersuneq fjord, high abundances of Atlantic water foraminifera indicate a relatively strong WGC influence and warm conditions during the interval from 6200 to 5000 cal. yr BP (Lloyd et al., 2007). This reconstruction is also supported by a relatively warm water mollusc fauna from Orpigsoq fjord between 7500 and 5500 cal. yr BP (Donner and Jungner, 1975) which however also caused cool surface water temperatures and a more unstable ocean circulation of the Labrador Sea due to meltwater release from the Canadian Arctic (Sheldon et al., 2015; Sheldon et al., 2016; Solignac et al., 2011). Likewise, on the East Greenland shelf, Jennings et al. (2002) detected a relatively weak EGC from the early Holocene until ca. 4700 cal. yr BP on the basis of foraminiferal data. After the onset of the mid-Holocene the IC cooled and/or weakened on the Greenland shelf (Andresen et al., 2013). Compiling Holocene marine and terrestrial records from the

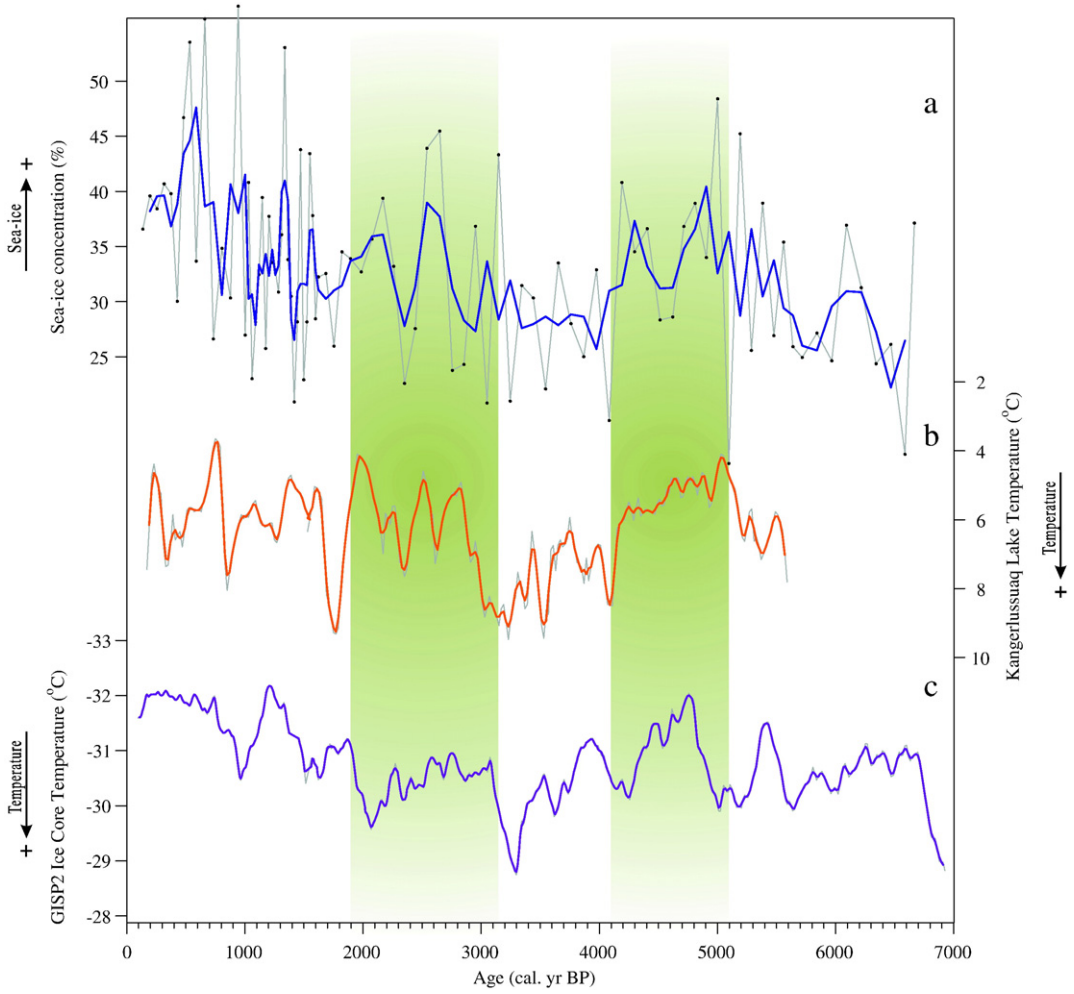

Fig. 4. Diatom-based sea-ice concentration reconstruction from core GA306-GC3 (blue curve). Alkenone-based Kangerlussuaq lake water temperature reconstruction (red curve) (D'Andrea et al., 2011). The GISP2 (Greenland Summit) ice core temperature reconstruction (purple curve) (Alley, 2000; Cuffey and Clow, 1997). Actual data are shown as grey lines; smoothed records (3-point running average) are denoted by bold lines in colour. Shaded areas show high sea-ice cover intervals at 5000–4100 cal. yr BP and 3100–2000 cal. yr BP.

Denmark Strait region, Andresen and Björck (2005) noted the initial onset of mid-Holocene climatic deterioration around 5000 cal. yr BP, followed by further climatic deterioration around 3500 cal. yr BP. The low sea-ice conditions before the mid-Holocene in our sea-ice reconstruction were also observed in a recent study from the North Icelandic Shelf, which showed low values of sea-ice proxies IP_{25} and quartz in cores MD99-2269 and JR51-GC35 during ca. 8000–5500 cal. yr BP, and a generally increasing trend during the late Holocene (Cabedo-Sanz et al., 2016).

The upper part of the sea-ice record, corresponding to the late Holocene (<3100 cal. yr BP), is marked by a gradual increase in sea-ice cover (Fig. 4a). The occurrence of this Neoglacial cooling, recognized in all three records (Fig. 4), is also supported by foraminiferal assemblages from the same core (GA306-GC3), which indicate an increased influence of polar waters from the EGC after 2900 cal. yr BP (Erbs-Hansen et al., 2013). There are differences in the timing of the beginning of the Neoglacial cooling in different records from along the West Greenland coast, but the estimates generally lie within the interval from 3500 to 2000 cal. yr BP (e.g. Lloyd et al., 2007; Moros et al., 2006; Ribeiro et al., 2012; Seidenkrantz et al., 2007, 2008). A similar scenario is also recognized in northernmost Baffin Bay, where the disappearance of calcareous foraminifera at ca. 3000 cal. yr BP (Knudsen et al., 2008), as well as a generally longer sea-ice season after 3600 cal. yr BP (Levac et al., 2001), indicates a decrease in surface water temperature. Furthermore, in the central Canadian Arctic Archipelago, elevated IP_{25} values indicate relatively more intensive spring sea-ice occurrences, beginning at ca. 3500–3000 cal. yr BP (Belt et al., 2010; Vare et al., 2009). Marine archives from East and Southeast Greenland also show that the Neoglacial interval was cold and variable after 3500 cal. yr BP, caused by a reduced influence of Atlantic-sourced water and increased freshwater forcing from the Arctic Ocean, coinciding with a southward advance of the Polar Front, and an advance of the Greenland Ice Sheet (Andresen et al., 2013; Jennings et al., 2011; Larsen et al., 2015), while ice sheet melting in the Canadian Arctic became reduced (Sheldon et al., 2015; Sheldon et al., 2016; Solignac et al., 2011). In the North Atlantic a cooling was also identified at ca. 3300 cal. yr BP (Koç Karpuz et al., 1993; as 3000 ^{14}C yr BP), and off North Iceland Cabedo-Sanz et al. (2016) identified a progressively cooler interval, with increasing influences from cold Polar water and drift ice delivered by the EGC during the late Holocene (ca. 3300 cal. yr BP to present).

We conclude that the similarity between the sea-ice variations off West Greenland and independent palaeoclimate records from Greenland and the wider Labrador region suggests that our findings are representative of a broad geographic area. Consequently, they enable us to evaluate possible contributions of different forcing factors to the reconstructed Holocene sea-ice conditions off West Greenland.

3.3. Potential forcing factors

Climate variations may be driven by a large number of factors, such as external forcing (e.g., solar variability and volcanism) (McGregor et al., 2015; Robock, 2000; Shindell et al., 2003; Sigl et al., 2015; Stoffel et al., 2015) and internal variability (e.g. natural changes in ocean circulation and natural oscillations in the coupled ocean-atmosphere system) (Bianchi and McCave, 1999; Knudsen et al., 2011; Mjell et al., 2015; Sorrel et al., 2012; Thornalley et al., 2009). Likely climate is a response to a combination of various triggering mechanism, but the significance of each mechanism may vary over time. Comparison of empirical proxy-based reconstructions with estimated forcing changes may improve our understanding of these factors governing climate changes.

3.3.1. External forcing

The Sun is the energy source that drives Earth's climate system, and it has been suggested that the forcing of centennial- to millennial-scale climate change during the Holocene was dominated by solar variability (Denton and Karlén, 1973; Gray et al., 2010; Rind, 2002; van Geel et al., 1999). Solar activity has also been proposed as the driver of oceanographic conditions in the North Atlantic, including temperature, ocean circulation and iceberg transport (Andrews et al., 2003; Bond et al., 2001; Knudsen et al., 2014; Moffa-Sánchez et al., 2014; Sejrup et al., 2010). In addition, our previous sea-ice proxy records and modelling results have demonstrated a general link between sea-ice cover off West Greenland and solar variability during the last millennium (Sha et al., 2016). Our modelling results show a strong negative correlation between sea-ice and solar variability along the eastern and southwestern coast of Greenland and in the Arctic Ocean, which indicates that solar variability has a significant effect on local sea-ice production (Sha et al., 2016) (Supplementary Fig. S3).

The sea-ice reconstruction for core GA306-GC3 has been compared with a record of the ^{14}C production rate, a proxy for past solar variability inferred from atmospheric ^{14}C concentrations measured in tree rings (Muscheler et al., 2007; Reimer et al., 2009) (Fig. 5). Calculation of Pearson's correlation coefficient for the sea-ice reconstruction versus ^{14}C production yields a positive correlation ($R = 0.35$; $P < 0.005$), and thus a statistically significant relationship between our sea-ice reconstruction and solar activity for the past 5000 yr. However, the correlation is much weaker for the interval prior to 5000 cal. yr BP ($R = 0.18$; $P < 0.005$) (Fig. 5). Furthermore, a cross wavelet analysis exhibits quite similar patterns (Supplementary Figs. S1 and S2). This suggests that during the Holocene a close relationship existed between solar activity and West Greenland sea ice over the past 5000 yr, but that the relationship was less obvious prior to 5000 cal. yr BP (Fig. 5).

Volcanic eruptions are another important external forcing factor driving climate changes, because their sulfate aerosol injections into the stratosphere shield the Earth's surface from incoming solar radiation, leading to short-term cooling at regional to global scale (Robock, 2000; Sigl et al., 2015). However, our sea-ice reconstructions do not demonstrate a relationship with known volcanic eruptions.

3.3.2. Ocean circulation

Oceanographic investigations have revealed the existence of two different sources or mechanism of sea-ice formation off West Greenland—local sea-ice and multi-year ice. The amount of multi-year ice off West Greenland, which is transported from the Arctic Ocean by the EGC and continues northwards assisted by the WGC, is linked not only to the outflow of sea ice from the Arctic Ocean (Buch, 2002), but also to the strength of ocean circulation in the North Atlantic.

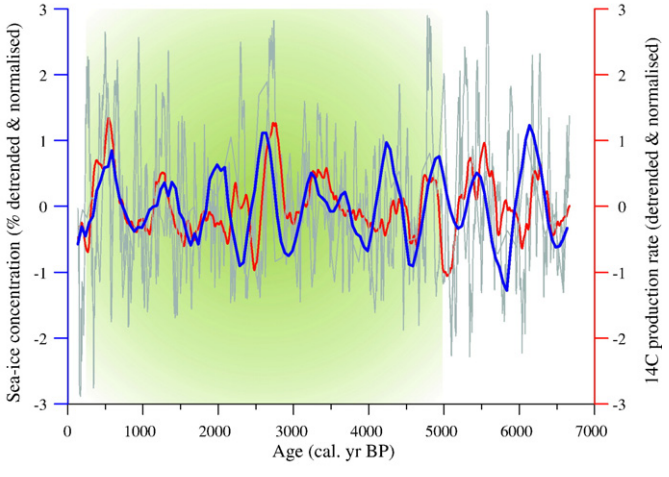

Fig. 5. Comparison of the detrended and normalized sea-ice concentration record (blue) and ^{14}C production rate (red) (Muscheler et al., 2007; Reimer et al., 2009). In order to remove high-frequency noise and long-term trends, both records were band-pass filtered for frequencies higher than 1/500 yr and lower than 1/2000 yr. The shaded area shows the interval with a high correlation between the two records during the last 5000 yr.

In order to assess a possible link between sea-ice variability at our study site in West Greenland, and the relative strength of the two different water mass components of the WGC (the EGC and the IC) throughout the Holocene, we plot the sea-ice reconstruction together with the abundance of benthic foraminifera *Elphidium excavatum* f. *clavata* and *Cassidulina reniforme* from the same core GA306-GC3 (at ca. 65-yr temporal resolution) (Erbs-Hansen et al., 2013) (Fig. 6).

The cold water benthic foraminifera *E. excavatum* f. *clavata*, which is abundant in glacial-marine environments and which tolerates unstable environmental conditions and somewhat reduced salinities, is believed to represent the influence of Polar water in the WGC at subsurface depths (Erbs-Hansen et al., 2013; Hald et al., 1994). In contrast, the benthic foraminifera *C. reniforme*, which requires fairly cold but more stable conditions, has been considered an indicator of cooled Atlantic water in the Disko Bugt region (Perner et al., 2011, 2013). *Cassidulina reniforme* may thus be regarded as an indicator of the contribution of the Atlantic water (IC) component to the WGC in our study. Therefore, the evolution of different water masses through time can be inferred based on the abundance of benthic foraminifera. For example, the upwards-increasing trend in the reconstructed sea-ice concentration, together with the high abundance of *E. excavatum* f. *clavata*, indicates the stronger influence of cold, lower salinity Polar water throughout the water column during the late Holocene, coinciding with a decrease in the influence of Atlantic water as inferred by decreasing abundance of *C. reniforme* (Fig. 6).

As illustrated in Fig. 6, the sea-ice reconstruction for the last ca. 6700 yr reveals a positive correlation with the abundance of the Polar water benthic foraminifera *E. excavatum* f. *clavata* ($R = 0.29$; $P < 0.005$, Fig. 6b); and a significant negative correlation with the abundance of *C. reniforme* ($R = -0.38$; $P < 0.005$, Fig. 6a). A cross-correlation analyses further indicates that the strongest correlations are obtained at almost zero lag (Supplementary Figs. S6 and S7). This indicates that sea-ice conditions off West Greenland are influenced by changes in the relative strength of the two components of the WGC, the cold Polar water from the EGC and the relatively warm Atlantic water from the IC. Similarly, the IP_{25} sea-ice proxy record from Fram Strait, and the May sea-ice reconstructions from the North Icelandic shelf, indicate an association between sea-ice cover and changes in the advection of relatively warm Atlantic and cold Polar water masses (Justwan and Koç Karpuz, 2008; Müller et al., 2012).

Climate modelling results demonstrate that, during intervals of low solar forcing, increased formation of sea ice in the Arctic may cause an increased export of sea ice and freshwater from the Arctic Ocean, which may be linked to the global thermohaline circulation via deep water formation in the North Atlantic (Lehner et al., 2013; Sha et al., 2016). In this scenario, the strength of the EGC plays a primary role in the advection of freshwater from the Arctic Ocean into the North Atlantic (Birchfield, 1993). The increased transport of Arctic sea ice and freshwater by the EGC in turn affects the ocean circulation in the North Atlantic and the intensity of deep-water masses through ocean convection in the Greenland Sea and Labrador Sea, with major implications for the Atlantic Meridional Overturning Circulation (Blaschek et al., 2015; Miettinen et al., 2015; Schmith and Hansen, 2003; Yu et al., 2016).

Organic geochemical analyses of Holocene marine sediment cores from Fram Strait further indicate that weak orbital forcing and reduced short-term Atlantic water advection promoted increased sea-ice coverage, representing a signature of sea-ice export from the Arctic Ocean, particularly during the late Holocene (Müller et al., 2012). This observation agrees with the record of overall increasing sea-ice concentration off West Greenland during the Neoglacial cooling (Fig. 6). Variations in solar activity may account for short-term variations in sea ice

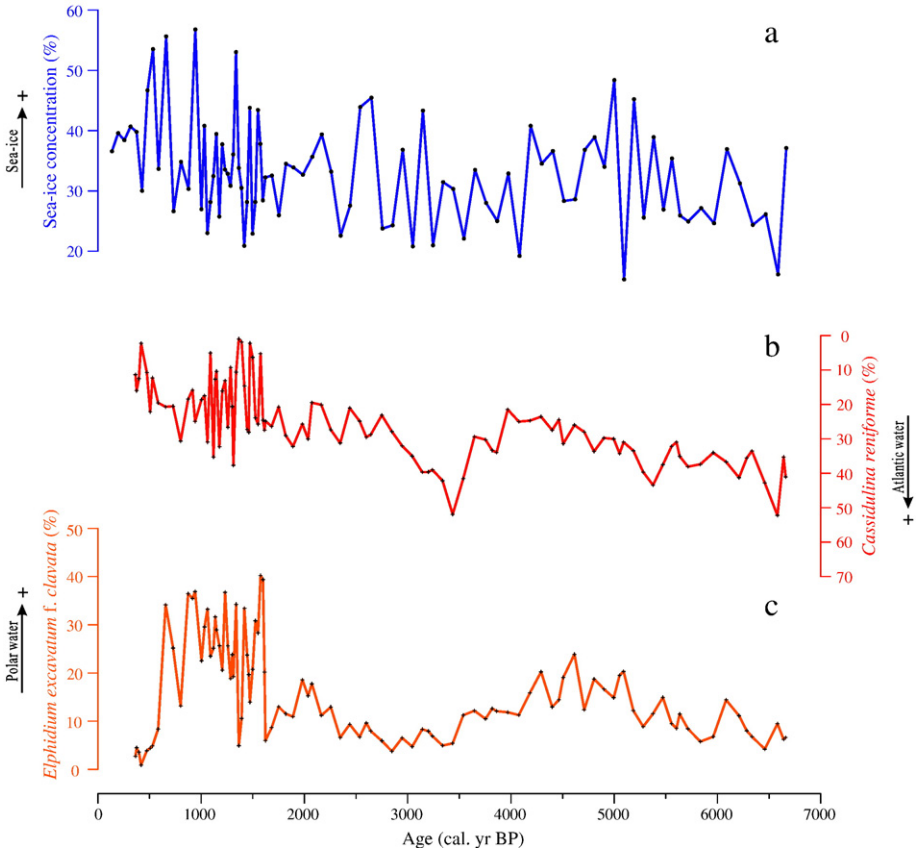

Fig. 6. Reconstructed sea-ice concentration (blue curve) compared to the abundance of selected benthic foraminiferal taxa *E. excavatum* f. *clavata* (orange curve) and *Cassidulina reniforme* (red curve) from the same core GA306-GC3 (Erbs-Hansen et al., 2013).

modifying the general pattern (Sha et al., 2016). The sea-ice extent, linked to changes in ocean circulation, e.g., the strength of the EGC, may also reveal either a strengthened or weakened thermohaline circulation (Müller et al., 2012).

It is noteworthy that prior to 5000 yr ago the abundances of the benthic foraminifera *E. excavatum* f. *clavata* and *C. reniforme* were significantly correlated with sea-ice records ($R = 0.36$, $P < 0.005$ and $R = -0.31$, $P < 0.005$, respectively; Fig. 6). This indicates that during this interval there was a strong link between sea-ice cover and ocean circulation (i.e. strength of the WGC). This strong link to ocean circulation may explain the clearly weaker correlation between solar activity and sea-ice records during this period ($R = 0.18$, $P < 0.005$). The weaker link between climate variability and solar irradiation has also been recognized during the early to mid-Holocene (>4000 cal. yr BP) for reconstructed summer sea-surface temperatures in the northern North Atlantic (Jiang et al., 2015). The interval from 7000 to 5000/4000 cal. yr BP was the least glacially-influenced phase of the Holocene and even most alpine areas had reached a stage of glacial minimum. During such warmer-than-present conditions, the still strong summer insolation resulted in a vigorous Atlantic Meridional Overturning Circulation and a more northerly position of the Intertropical Convergence Zone (Haug et al., 2001; Mayewski et al., 2004), which may have weakened the influence of solar irradiation variability on the North Atlantic (Renssen et al., 2006). Therefore, changes in insolation had a minor effect on the sea-ice cover during this period, whereas the ocean circulation was a more important factor controlling sea-ice variability. After the mid-Holocene, climatic cooling led to a weaker Atlantic Meridional Overturning Circulation and a southward movement of the Intertropical Convergence Zone (Mayewski et al., 2004; Jiang et al., 2015), amplifying the solar influence on the climate system (Jiang et al., 2015). However, Debret et al. (2009) indicated that Holocene palaeoclimatic records exhibit a ~1500 yr cycle during the mid-Holocene, which might be related to thermohaline circulation forcing.

Imbalances in solar radiation drive global ocean circulation; however, ocean circulation plays a key role in distributing solar energy and maintaining climate (Haigh, 2011). Solar activity seems to play a more important role in modulating sea ice during periods of somewhat weaker thermohaline circulation (<5000/4000 cal. yr BP), while a stronger thermohaline circulation overprints solar activity, reducing the impact of solar forcing on climate.

4. Conclusions

Holocene sea-ice variability off West Greenland has been reconstructed by applying a sea-ice transfer function to diatom data from gravity core GA306-GC3 from Holsteinsborg Dyb, which spans the last ca. 6700 yr. The reconstruction indicates warm conditions with reduced sea-ice cover, associated with the Holocene Thermal Maximum, from ca. 6700 to 5000 cal. yr BP. Cold conditions and persistent sea-ice cover occurred from 5000 to 4000 cal. yr BP, followed by a decrease in sea-ice cover from 4000 to 3200 cal. yr BP. A subsequent gradual increase in sea-ice cover from 3200 cal. yr BP corresponds to the well-documented Northern Hemisphere cooling of the Neoglacial. A distinct increase in sea-ice cover began at 1750 cal. yr BP, with absolute maximum values during the last millennium.

Our sea-ice reconstruction is in broad agreement with the alkenone-based temperature reconstruction from two lakes in the Kangerlussuaq region and with the temperature record from the GISP2 ice core from the Greenland Summit, which suggests that our findings are representative of a broad geographic area.

In order to assess the contribution of different potential forcing factors to sea-ice conditions off West Greenland, we evaluated the relationship between our sea-ice reconstruction and solar activity, as well as with the strength of ocean circulation. The observed agreement between the sea-ice record and solar activity suggests that solar forcing may have been an important trigger for sea-ice variability off West Greenland during the last 5000 yr. In addition, the variability of sea-ice conditions within the region was also linked to changes in the strength of two different water masses (cold Polar water from the EGC and warm Atlantic water from the IC, respectively) during the past ca. 7000 yr, especially prior to 5000 cal. yr BP. Overall, the reconstructed sea-ice proxy record presented here, which is also supported by modelling results, suggests that solar activity combined with ocean circulation has a considerable impact on climate change on a longer-time scale.

Acknowledgments

The core material was obtained from the *Galathea 3 Expedition* cruise in 2006. We are grateful to the captain, crew and expedition members for coring and seismic operations on board HMS *Vædderen* and all cruises providing surface samples for our study. We thank Jan Heinemeier, Aarhus University, Denmark, for providing the ^{14}C age determinations and Thorbjørn Joest Andersen, University of Copenhagen, Denmark, for the ^{210}Pb datings. Financial support for this work was provided by the Natural Science Foundation of China (Grants 41406209, 41176048, 41302134, U1609203), the Natural Science Foundation of Zhejiang Province (Grant LY17D060001), the Chinese polar environment comprehensive investigation & assessment programmes (Grant CHINARE2017-03-02), and the European Union's Seventh Framework programme (FP7/2007e2013) "Past4Future" Climate Change - Learning from the past climate (Grant 243908), as well as K.C. Wong Magna Fund in Ningbo University. This work is also a contribution to the PAGES sea-ice proxy (SIP) working group and the Taishan Scholars Program of Shandong. Finally, we are grateful to two anonymous referees and the Editor, Prof. Thierry Corrège for the constructive and useful comments.

Appendix A. Supplementary data

Supplementary data to this article can be found online at http://dx.doi.org/10.1016/j.palaeo.2017.03.022.

References

Alley, R.B., 2000. The Younger Dryas cold interval as viewed from central Greenland. Quat. Sci. Rev. 19, 213–226.
Andresen, C.S., Björck, S., 2005. Holocene climate variability in the Denmark Strait region - a land-sea correlation of new and existing climate proxy records. Geogr. Ann. A: Phys. Geogr. 87, 159–174.
Andresen, C.S., Hansen, M.J., Seidenkrantz, M.-S., Jennings, A.E., Knudsen, M.F., Nørgaard-Pedersen, N., Larsen, N.K., Kuijpers, A., Pearce, C., 2013. Mid- to late-Holocene oceanographic variability on the Southeast Greenland shelf. The Holocene 23, 167–178.
Andrews, J.T., Hardadottir, J., Stoner, J.S., Mann, M.E., Kristjansdottir, G.B., Koç Karpuz, N., 2003. Decadal to millennial-scale periodicities in North Iceland shelf sediments over the last 12,000 cal yr: long-term North Atlantic oceanographic variability and solar forcing. Earth Planet. Sci. Lett. 210, 453–465.
Bauch, H.A., Polyakova, Y.I., 2000. Late Holocene variations in Arctic shelf hydrology and sea-ice regime: evidence from north of the Lena Delta. Int. J. Earth Sci. 89, 569–577.
Belt, S.T., Müller, J., 2013. The Arctic sea ice biomarker IP25: a review of current understanding, recommendations for future research and applications in palaeo sea ice reconstructions. Quat. Sci. Rev. 79, 9–25.
Belt, S.T., Massé, G., Rowland, S.J., Poulin, M., Michel, C., LeBlanc, B., 2007. A novel chemical fossil of palaeo sea ice: IP25. Org. Geochem. 38, 16–27.
Belt, S.T., Vare, L.L., Massé, G., Manners, H.R., Price, J.C., MacLachlan, S.E., Andrews, J.T., Schmidt, S., 2010. Striking similarities in temporal changes to spring sea ice occurrence across the central Canadian Arctic Archipelago over the last 7000 years. Quat. Sci. Rev. 29, 3489–3504.
Bianchi, G.G., McCave, I.N., 1999. Holocene periodicity in North Atlantic climate and deep-ocean flow south of Iceland. Nature 397, 515–517.
Birchfield, G.E., 1993. Comments on "two stable equilibria of a coupled ocean-atmosphere model". J. Clim. 6, 175–177.
Blaschek, M., Bakker, P., Renssen, H., 2015. The influence of Greenland ice sheet melting on the Atlantic meridional overturning circulation during past and future warm periods: a model study. Clim. Dyn. 44, 2137–2157.
Bond, G., Kromer, B., Beer, J., Muscheler, R., Evans, M.N., Showers, W., Hoffmann, S., Lotti-Bond, R., Hajdas, I., Bonani, G., 2001. Persistent solar influence on North Atlantic climate during the Holocene. Science 294, 2130–2136.
Buch, E., 2000. A Monograph on the Physical Oceanography of the Greenland Waters. Danish Meteorological Institute Scientific Report, Copenhagen, pp. 1–405.
Buch, E., 2002. Present Oceanographic Conditions in Greenland Waters. Danish Meteorological Institute Scientific Report, Copenhagen, pp. 1–36.

Buch, E., Nielsen, M.H., 2001. Oceanographic investigations of West Greenland 2000. In: Organization, N.A.F (Ed.), NAFO Scientific Council Documents, pp. 1–23.
Cabedo-Sanz, P., Belt, S.T., Jennings, A.E., Andrews, J.T., Geirsdóttir, Á., 2016. Variability in drift ice export from the Arctic Ocean to the North Icelandic Shelf over the last 8000 years: a multi-proxy evaluation. Quat. Sci. Rev. 146, 99–115.
Cremer, H., 1998. The diatom flora of the Laptev Sea (Arctic Ocean). Bibl. Diatomol. 40, 5–169.
Cuffey, K.M., Clow, G.D., 1997. Temperature, accumulation, and ice sheet elevation in central Greenland through the last deglacial transition. J. Geophys. Res. 102, 26383–26396.
Cuny, J., Rhines, P.B., Niiler, P.P., Bacon, S., 2002. Labrador Sea Boundary Currents and the Fate of the Irminger Sea Water. J. Phys. Oceanogr. 32, 627–647.
D'Andrea, W.J., Huang, Y., Fritz, S.C., Anderson, N.J., 2011. Abrupt Holocene climate change as an important factor for human migration in West Greenland. Proc. Natl. Acad. Sci. U. S. A. 108, 9765–9769.
de Vernal, A., Hillaire-Marcel, C., 2000. Sea-ice cover, sea-surface salinity and halo-/thermocline structure of the northwest North Atlantic: modern versus full glacial conditions. Quat. Sci. Rev. 19, 65–85.
de Vernal, A., Hillaire-Marcel, C., Rochon, A., Fréchette, B., Henry, M., Solignac, S., Bonnet, S., 2013a. Dinocyst-based reconstructions of sea ice cover concentration during the Holocene in the Arctic Ocean, the northern North Atlantic Ocean and its adjacent seas. Quat. Sci. Rev. 79, 111–121.
de Vernal, A., Rochon, A., Fréchette, B., Henry, M., Radi, T., Solignac, S., 2013b. Reconstructing past sea ice cover of the Northern Hemisphere from dinocyst assemblages: status of the approach. Quat. Sci. Rev. 79, 122–134.
Debret, M., Sebag, D., Crosta, X., Massei, N., Petit, J.R., Chapron, E., Bout-Roumazeilles, V., 2009. Evidence from wavelet analysis for a mid-Holocene transition in global climate forcing. Quat. Sci. Rev. 28, 2675–2688.
Denton, G.H., Karlén, W., 1973. Holocene climatic variations—their pattern and possible cause. Quat. Res. 3, 155–205.
Donner, J., Jungner, H., 1975. Radiocarbon dating of shells from marine Holocene deposits in the Disko Bugt area, West Greenland. Boreas 4, 25–45.
Erbs-Hansen, D.R., Knudsen, K.L., Olsen, J., Lykke-Andersen, H., Underbjerg, J.A., Sha, L., 2013. Paleoceanographical development off Sisimiut, West Greenland, during the mid- and late Holocene: a multiproxy study. Mar. Micropaleontol. 102, 79–97.
Funder, S., Goosse, H., Jepsen, H., Kaas, E., Kjær, K.H., Korsgaard, N.J., Larsen, N.K., Linderson, H., Lyså, A., Möller, P., Olsen, J., Willerslev, E., 2011. A 10,000-year record of Arctic Ocean sea-ice variability—view from the beach. Science 333, 747–750.
Funder, S., Weidick, A., 1991. Holocene boreal molluscs in Greenland — palaeoceanographic implications. Palaeogeogr. Palaeocl. 85, 123–135.
Gajewski, K., 2015. Quantitative reconstruction of Holocene temperatures across the Canadian Arctic and Greenland. Glob. Planet. Chang. 128, 14–23.
Gray, L.J., Beer, J., Geller, M., Haigh, J.D., Lockwood, M., Matthes, K., Cubasch, U., Fleitmann, D., Harrison, G., Hood, L., Luterbacher, J., Meehl, G.A., Shindell, D., van Geel, B., White, W., 2010. Solar influence on climate. Rev. Geophys. 48, RG4001.
Haigh, J.D., 2011. Solar Influences on Climate, Briefing Paper No. 5. Grantham Institute for Climate Change, pp. 1–20.
Hald, M., Steinsund, P.I., Dokken, T., Korsun, S., Polyak, L., Aspeli, R., 1994. Recent and late quaternary distribution of the *Elphidium excavatum* f. *clavata* in Arctic seas. Cushman Found. Spec. Publ. 32, 141–153.
Hansen, K.Q., Buch, E., Gregersen, U., 2004. Weather, Sea and Ice Conditions Offshore West Greenland – Focusing on New License Areas 2004. Danish Meteorological Institute Scientific Report, Copenhagen, pp. 1–31.
Hasle, G.R., Syvertsen, E.E., 1997. Marine diatoms. In: Tomas, C.R. (Ed.), Identifying Marine Phytoplankton. Academic Press, San Diego, pp. 5–385.
Haug, G.H., Hughen, K.A., Sigman, D.M., Peterson, L.C., Röhl, U., 2001. Southward migration of the Intertropical Convergence Zone through the Holocene. Science 293, 1304–1308.
Holland, M.M., Bitz, C.M., Tremblay, B., 2006. Future abrupt reductions in the summer Arctic sea ice. Geophys. Res. Lett. 33, L23503.
Jennings, A., Andrews, J., Wilson, L., 2011. Holocene environmental evolution of the SE Greenland Shelf North and South of the Denmark Strait: Irminger and East Greenland current interactions. Quat. Sci. Rev. 30, 980–998.
Jennings, A.E., Knudsen, K.L., Hald, M., Hansen, C.V., Andrews, J.T., 2002. A mid-Holocene shift in Arctic sea-ice variability on the East Greenland Shelf. The Holocene 12, 49–58.
Jensen, K.G., 2003. Holocene hydrographic changes in Greenland coastal waters. Reconstructing Environmental Change from Sub-fossil and Contemporary Diatoms. Faculty of Science, University of Copenhagen, Copenhagen, pp. 1–160.
Jiang, H., Eiríksson, J., Schulz, M., Knudsen, K.L., Seidenkrantz, M.-S., 2005. Evidence for solar forcing of sea-surface temperature on the North Icelandic Shelf during the late Holocene. Geology 33, 73–76.
Jiang, H., Muscheler, R., Björck, S., Seidenkrantz, M.-S., Olsen, J., Sha, L., Sjolte, J., Eiríksson, J., Ran, L., Knudsen, K.-L., Knudsen, M.F., 2015. Solar forcing of Holocene summer sea-surface temperatures in the northern North Atlantic. Geology 43, 203–206.
Jiang, H., Seidenkrantz, M.-S., Knudsen, K.L., Eiríkson, J., 2001. Diatom surface sediment assemblages around Iceland and their relationships to oceanic environmental variables. Mar. Micropaleontol. 41, 73–96.
Jones, P.D., Osborn, T.J., Briffa, K.R., 2001. The evolution of climate over the last millennium. Science 292, 662–667.
Justwan, A., Koç Karpuz, N., 2008. A diatom based transfer function for reconstructing sea ice concentrations in the North Atlantic. Mar. Micropaleontol. 66, 264–278.
Kaplan, M.R., Wolfe, A.P., Miller, G.H., 2002. Holocene environmental variability in Southern Greenland inferred from lake sediments. Quat. Res. 58, 149–159.
Kaufman, D.S., Ager, T.A., Anderson, N.J., Anderson, P.M., Andrews, J.T., Bartlein, P.J., Brubaker, L.B., Coats, L.L., Cwynar, L.C., Duvall, M.L., Dyke, A.S., Edwards, M.E., Eisner, W.R., Gajewski, K., Geirsdóttir, A., Hu, F.S., Jennings, A.E., Kaplan, M.R., Kerwin, M.W., Lozhkin, A.V., MacDonald, G.M., Miller, G.H., Mock, C.J., Oswald, W.W., Otto-Bliesner, B.L., Porinchu, D.F., Rühland, K., Smol, J.P., Steig, E.J., Wolfe, B.B., 2004. Holocene thermal maximum in the western Arctic (0–180°W). Quat. Sci. Rev. 23, 529–560.
Kinnard, C., Zdanowicz, C.M., Fisher, D.A., Isaksson, E., de Vernal, A., Thompson, L.G., 2011. Reconstructed changes in Arctic sea ice over the past 1,450 years. Nature 479, 509–512.
Knudsen, K.L., Stabell, B., Seidenkrantz, M.-S., Eiríksson, J., Blake Jr., W., 2008. Deglacial and Holocene conditions in northernmost Baffin Bay: sediments, foraminifera, diatoms and stable isotopes. Boreas 37, 346–376.
Knudsen, M.F., Jacobsen, B.H., Seidenkrantz, M.-S., Olsen, J., 2014. Evidence for external forcing of the Atlantic Multidecadal Oscillation since termination of the Little Ice Age. Nat. Commun. 5, 3323.
Knudsen, M.F., Seidenkrantz, M.-S., Jacobsen, B.H., Kuijpers, A., 2011. Tracking the Atlantic Multidecadal Oscillation through the last 8,000 years. Nat. Commun. 2, 178.
Koç Karpuz, N., Jansen, E., Haflidason, H., 1993. Paleoceanographic reconstructions of surface ocean conditions in the Greenland, Iceland and Norwegian seas through the last 14 ka based on diatoms. Quat. Sci. Rev. 12, 115–140.
Koç Karpuz, N., Schrader, H., 1990. Surface sediment diatom distribution and Holocene Paleotemperature variations in the Greenland, Iceland and Norwegian Sea. Paleoceanography 5, 557–580.
Krawczyk, D., Witkowski, A., Moros, M., Lloyd, J., Kuijpers, A., Kierzek, A., 2010. Late-Holocene diatom-inferred reconstruction of temperature variations of the West Greenland Current from Disko Bugt, central West Greenland. The Holocene 20, 659–666.
Larsen, N.K., Kjær, K.H., Lecavalier, B., Bjørk, A.A., Colding, S., Huybrechts, P., Jakobsen, K.E., Kjeldsen, K.K., Knudsen, K.L., Odgaard, B.V., Olsen, J., 2015. The response of the southern Greenland ice sheet to the Holocene thermal maximum. Geology 43, 291–294.
Lehner, F., Born, A., Raible, C.C., Stocker, T.F., 2013. Amplified inception of European Little Ice Age by sea ice–ocean–atmosphere feedbacks. J. Clim. 26, 7586–7602.
Levac, E., Vernal, A.D., Blake Jr., W., 2001. Sea-surface conditions in northernmost Baffin Bay during the Holocene: palynological evidence. J. Quat. Sci. 16, 353–363.
Lloyd, J.M., Kuijpers, A., Long, A., Moros, M., Park, L.A., 2007. Foraminiferal reconstruction of mid- to late-Holocene ocean circulation and climate variability in Disko Bugt, West Greenland. The Holocene 17, 1079–1091.
Müller, J., Wagner, A., Fahl, K., Stein, R., Prange, M., Lohmann, G., 2011. Towards quantitative sea ice reconstructions in the northern North Atlantic: a combined biomarker and numerical modelling approach. Earth Planet. Sci. Lett. 306, 137–148.
Müller, J., Werner, K., Stein, R., Fahl, K., Moros, M., Jansen, E., 2012. Holocene cooling culminates in sea ice oscillations in Fram Strait. Quat. Sci. Rev. 47, 1–14.
Massé, G., Belt, S.T., Sicre, M.-A., 2010. Arctic Sea Ice: High Resolution Reconstructions, Iceland in the Central Northern Atlantic: Hotspot, Sea Currents and Climate Change (Plouzané).
Massé, G., Rowland, S.J., Sicre, M.-A., Jacob, J., Jansen, E., Belt, S.T., 2008. Abrupt climate changes for Iceland during the last millennium: evidence from high resolution sea ice reconstructions. Earth Planet. Sci. Lett. 269, 565–569.
Mayewski, P.A., Rohling, E.E., Stager, J.C., Karlén, W., Maasch, K.A., Meeker, L.D., Meyerson, E.A., Gasse, F., van Kreveld, S., Holmgren, K., Lee-Thorp, J.A., Rosqvist, G., Rack, F., Staubwasser, M., Schneider, R.R., Steig, E.J., 2004. Holocene climate variability. Quat. Res. 62, 243–255.
McGregor, H.V., Evans, M.N., Goosse, H., Leduc, G., Martrat, B., Addison, J.A., Mortyn, P.G., Oppo, D.W., Seidenkrantz, M.-S., Sicre, M.-A., Phipps, S.J., Selvaraj, K., Thirumalai, K., Filipsson, H.L., Ersek, V., 2015. Robust global ocean cooling trend for the pre-industrial Common Era. Nat. Geosci. 8, 671–677.
McNeely, R., Dyke, A.S., Southon, J.R., 2006. Canadian Marine Reservoir Ages, Preliminary Data Assessment. (Open file 5049 ed). Geological Survey of Canada.
Medlin, L.K., Priddle, J., 1990. Polar Marine Diatoms. Natural Environment Research Council, Cambridge.
Miettinen, A., Divine, D.V., Husum, K., Koç, N., Jennings, A., 2015. Exceptional ocean surface conditions on the SE Greenland shelf during the Medieval Climate Anomaly. Paleoceanography 30, 1657–1674.
Mjell, T.L., Ninnemann, U.S., Eldevik, T., Kleiven, H.K.F., 2015. Holocene multidecadal- to millennial-scale variations in Iceland-Scotland overflow and their relationship to climate. Paleoceanography 30, 558–569.
Moffa-Sánchez, P., Born, A., Hall, I.R., Thornalley, D.J.R., Barker, S., 2014. Solar forcing of North Atlantic surface temperature and salinity over the past millennium. Nat. Geosci. 7, 275–278.
Moros, M., Jensen, K.G., Kuijpers, A., 2006. Mid- to late-Holocene hydrological and climatic variability in Disko Bugt, central West Greenland. The Holocene 16, 357–367.
Muscheler, R., Joos, F., Beer, J., Müller, S.A., Vonmoos, M., Snowball, I., 2007. Solar activity during the last 1000 yr inferred from radionuclide records. Quat. Sci. Rev. 26, 82–97.
NSIDC (National Snow and Ice Data Centre), 2016. BIST: Browse Image Subset Tool. http://nsidc.org/data/bist/bist.pl?annot=1&legend=1&scale=75&tab_cols=2&tab_rows=2&config=seaice_extent_trends&submit=Refresh&hemis0=N&img0=trnd&hemis1=N&img1=plot&mo0=08&year0=2016&mo1=09&year1=2016.
Perner, K., Moros, M., Lloyd, J.M., Kuijpers, A., Telford, R.J., Harff, J., 2011. Centennial scale benthic foraminiferal record of late Holocene oceanographic variability in Disko Bugt, West Greenland. Quat. Sci. Rev. 30, 2815–2826.
Perner, K., Moros, M., Jennings, A., Lloyd, J., Knudsen, K., 2013. Holocene palaeoceanographic evolution off West Greenland. Holocene 23, 374–387.
Ramsey, C.B., 2009. Bayesian analysis of radiocarbon dates. Radiocarbon 51, 337–360.
Reed, J.M., Mesquita-Joanes, F., Griffiths, H.I., 2012. Multi-indicator conductivity transfer functions for Quaternary palaeoclimate reconstruction. J. Paleolimnol. 47, 251–275.
Reimer, P.J., Baillie, M.G.L., Bard, E., Bayliss, A., Beck, J.W., Blackwell, P.G., Ramsey, C.B., Buck, C.E., Burr, G.S., EDWARDS, R.L., Friedrich, M., Grootes, P.M., Guilderson, T.P., Hajdas, I., Heaton, T.J., Hogg, A.G., Hughen, K.A., Kaiser, K.F., Kromer, B., McCormac, F.G., Manning, S.W., Reimer, R.W., Richards, D.A., Southon, J.R., Talamo, S., Turney,

C.S.M., van der Plicht, J., Weyhenmeyer, C.E., 2009. IntCal09 and Marine09 radiocarbon age calibration curves, 0–50,000 years cal BP. Radiocarbon 51, 1111–1150.
Renssen, H., Goosse, H., Muscheler, R., 2006. Coupled climate model simulation of Holocene cooling events: oceanic feedback amplifies solar forcing. Clim. Past 2, 79–90.
Ribeiro, S., Moros, M., Ellegaard, M., Kuijpers, A., 2012. Climate variability in West Greenland during the past 1500 years: evidence from a high-resolution marine palynological record from Disko Bay. Boreas 41, 68–83.
Rind, D., 2002. The sun's role in climate variations. Science 296, 673–677.
Robock, A., 2000. Volcanic eruptions and climate. Rev. Geophys. 38, 191–219.
Schlitzer, R., 2011. Ocean Data View. http://odv.awi.de.
Schmith, T., Hansen, C., 2003. Fram Strait ice export during the nineteenth and twentieth centuries reconstructed from a multiyear sea ice index from Southwestern Greenland. J. Clim. 16, 2782–2791.
Schulz, M., Mudelsee, M., 2002. REDFIT: estimating red-noise spectra directly from unevenly spaced paleoclimatic time series. Comput. Geosci. 28, 421–426.
Seidenkrantz, M.-S., 2013. Benthic foraminifera as palaeo sea-ice indicators in the subarctic realm – examples from the Labrador Sea–Baffin Bay region. Quat. Sci. Rev. 79, 135–144.
Seidenkrantz, M.-S., Aagaard-Sørensen, S., Sulsbrück, H., Kuijpers, A., Jensen, K.G., Kunzendorf, H., 2007. Hydrography and climate of the last 4400 years in a SW Greenland fjord: implications for Labrador Sea palaeoceanography. The Holocene 17, 387–401.
Seidenkrantz, M.-S., Roncaglia, L., Fischel, A., Heilmann-Clausen, C., Kuijpers, A., Moros, M., 2008. Variable North Atlantic climate seesaw patterns documented by a late Holocene marine record from Disko Bugt, West Greenland. Mar. Micropaleontol. 68, 66–83.
Sejrup, H.P., Lehman, S.J., Haflidason, H., Noone, D., Muscheler, R., Berstad, I.M., Andrews, J.T., 2010. Response of Norwegian Sea temperature to solar forcing since 1000 A.D. J. Geophys. Res. 115, C12034.
Sha, L., Jiang, H., Liu, Y., Zhao, M., Li, D., Chen, Z., Zhao, Y., 2015. Palaeo-sea-ice changes on the North Icelandic shelf during the last millennium: evidence from diatom records. Sci. China Earth Sci. 58, 962–970.
Sha, L., Jiang, H., Seidenkrantz, M.-S., Knudsen, K.L., Olsen, J., Kuijpers, A., Liu, Y., 2014. A diatom-based sea-ice reconstruction for the Vaigat Strait (Disko Bugt, West Greenland) over the last 5000 yr. Palaeogeogr. Palaeocl. 403, 66–79.
Sha, L., Jiang, H., Seidenkrantz, M.-S., Muscheler, R., Zhang, X., Knudsen, M.F., Olsen, J., Knudsen, K.L., Zhang, W., 2016. Solar forcing as an important trigger for West Greenland sea-ice variability over the last millennium. Quat. Sci. Rev. 131, 148–156.
Sheldon, C.M., Seidenkrantz, M.-S., Frandsen, P., Jacobsen, H.V., Van Nieuwenhove, N., Solignac, S., Pearce, C., Palitzsch, M.G., Kuijpers, A., 2015. Variable inFlux of West Greenland Current Water into the Labrador Current Through the Last 7200 years: A Multiproxy Record from Trinity Bay (NE Newfoundland) (arktos 1, 8).
Sheldon, C.M., Seidenkrantz, M.-S., Pearce, C., Kuijpers, A., Hansen, M.J., Christensen, E.Z., 2016. Holocene oceanographic changes in SW Labrador Sea, off Newfoundland. The Holocene 26, 274–289.
Shindell, D.T., Schmidt, G.A., Miller, R.L., Mann, M.E., 2003. Volcanic and solar forcing of climate change during the preindustrial era. J. Clim. 16, 4094–4107.
Sigl, M., Winstrup, M., McConnell, J.R., Welten, K.C., Plunkett, G., Ludlow, F., Buntgen, U., Caffee, M., Chellman, N., Dahl-Jensen, D., Fischer, H., Kipfstuhl, S., Kostick, C., Maselli, O.J., Mekhaldi, F., Mulvaney, R., Muscheler, R., Pasteris, D.R., Pilcher, J.R., Salzer, M., Schupbach, S., Steffensen, J.P., Vinther, B.M., Woodruff, T.E., 2015. Timing and climate forcing of volcanic eruptions for the past 2,500 years. Nature 523, 543–549.
Solignac, S., Seidenkrantz, M.-S., Jessen, C., Kuijpers, A., Gunvald, A.K., Olsen, J., 2011. Late-Holocene sea-surface conditions offshore Newfoundland based on dinoflagellate cysts. The Holocene 21, 539–552.
Sorrel, P., Debret, M., Billeaud, I., Jaccard, S.L., McManus, J.F., Tessier, B., 2012. Persistent non-solar forcing of Holocene storm dynamics in coastal sedimentary archives. Nat. Geosci. 5, 892–896.
Stoffel, M., Khodri, M., Corona, C., Guillet, S., Poulain, V., Bekki, S., Guiot, J., Luckman, B.H., Oppenheimer, C., Lebas, N., Beniston, M., Masson-Delmotte, V., 2015. Estimates of volcanic-induced cooling in the Northern Hemisphere over the past 1,500 years. Nat. Geosci. 8, 784–788.
Stroeve, J.C., Serreze, M.C., Holland, M.M., Kay, J.E., Malanik, J., Barrett, A.P., 2012. The Arctic's rapidly shrinking sea ice cover: a research synthesis. Clim. Chang. 110, 1005–1027.
Tang, C.C.L., Ross, C.K., Yao, T., Petrie, B., DeTracey, B.M., Dunlap, E., 2004. The circulation, water masses and sea-ice of Baffin Bay. Prog. Oceanogr. 63, 183–228.
Thornalley, D.J.R., Elderfield, H., McCave, I.N., 2009. Holocene oscillations in temperature and salinity of the surface subpolar North Atlantic. Nature 457, 711–714.
Torrence, C., Compo, G.P., 1998. A practical guide to wavelet analysis. Bull. Amer. Meteor. Soc. 79, 61–78.
van Geel, B., Raspopov, O.M., Renssen, H., van der Plicht, J., Dergachev, V.A., Meijer, H.A.J., 1999. The role of solar forcing upon climate change. Quat. Sci. Rev. 18, 331–338.
Vare, L.L., Massé, G., Gregory, T.R., Smart, C.W., Belt, S.T., 2009. Sea ice variations in the central Canadian Arctic Archipelago during the Holocene. Quat. Sci. Rev. 28, 1354–1366.
von Quillfeldt, C.H., 1996. Ice algae and phytoplankton in north Norwegian and Arctic waters. Species Composition, Succession and Distribution. University of Tromsø, pp. 1–250.
Wang, M., Overland, J.E., 2012. A sea ice free summer Arctic within 30 years: an update from CMIP5 models. Geophys. Res. Lett. 39, L18501.
Weckström, K., Massé, G., Collins, L.G., Hanhijärvi, S., Bouloubassi, I., Sicre, M.-A., Seidenkrantz, M.-S., Schmidt, S., Andersen, T.J., Andersen, M.L., Hill, B., Kuijpers, A., 2013. Evaluation of the sea ice proxy IP25 against observational and diatom proxy data in the SW Labrador Sea. Quat. Sci. Rev. 79, 53–62.
Witkowski, A., Lange-Bertalot, H., Metzeltin, D., 2000. Diatom flora of marine coasts. In: Lange-Bertalot, H. (Ed.), Iconographia diatomologica. A.R.G. Gantner, p. 925.
Yu, L., Gao, Y., Otterå, O.H., 2016. The sensitivity of the Atlantic meridional overturning circulation to enhanced freshwater discharge along the entire, eastern and western coast of Greenland. Clim. Dyn. 46, 1351–1369.